Supporting Information

Tseng et al. 10.1073/pnas.1417989112

SI Methods

Tissue Preparation and Immunohistochemistry. Mice at postnatal day 24 were anesthetized and killed by cardiac perfusion before removal of their brains and fixation in 4% (wt/vol) paraformaldehyde overnight. Tissue was dehydrated through a standard paraffin embedding protocol using increasing concentrations of ethanol followed by clearing in xylene and infiltration with molten paraffin in a vacuum oven. For long term storage and preservation, paraffin sections were cut at 7 μm using a Leica RM2155 rotary microtome and then mounted onto microscope slides. Embedding material was removed by Histo-Clear (VWR) and rehydrated using decreasing concentrations of ethanol followed by PBS. For antigen retrieval, samples were boiled for 20 min in 10 mM sodium citrate. Slides were then cooled, washed in PBS, blocked using blocking buffer [5% (wt/vol) fish skin gelatin in PBS containing 0.1% Triton X-100], and incubated with primary antibodies in blocking buffer. On the following day, sections were washed by PBS-0.2% Tween 20 (Calbiochem) (PBST) and incubated with secondary fluorescent antibodies in blocking buffer at room temperature for 2 h. Finally, sections were washed in PBST, mounted with Prolong Gold Antifade reagent (Life Technologies), edges sealed with nail polish, and stored at 4 °C.

DNA Constructs. 190 kDa (1) and 480 kDa (2) ankyrin-G–GFP were previously described. W1989R 480-kDa ankyrin-G–GFP was generated using the Quikchange II XL mutagenesis kit (Agilent). CAG-Cre-2A-BFP plasmid was generated by cloning a Cre recombinase, a viral 2A peptide, and a TagBFP (a gift from James Bear, University of North Carolina, Chapel Hill) into pLenti6-V5-DEST viral vector (Invitrogen) with its promoter replaced by CAG (a gift from Scott Soderling, Duke University). CAG-pEGFP-N1 plasmid was acquired by replacing CMV promoter from pEGFP-N1 (Addgene) with CAG promoter. CAG-pEBFP-N1 plasmid was generated by replacing GFP with TagBFP in CAG-pEGFP-N1 vector. CAG-Cre-2A-GFP plasmid was obtained by cloning a Cre and a 2A peptide into CAG-pEGFP-N1 vector. Full-length GABARAP was pulled out from mouse brain library using yeast two-hybrid and cloned into pGEX/MAL expression vector. WT or W1989R giant insert region from residue 1819–2535 was cloned into pGEX/MAL expression vector.

Antibodies. Rabbit anti–480-kDa ankyrin-G (2), rabbit anti–beta-4 spectrin (2), goat anti–C-terminal (total) ankyrin-G (3), rabbit anti-neurofascin FNIII (4), and rabbit anti-GFP (5) antibodies were previously described. Rabbit anti-beta-2 spectrin antibody was generated using an epitope consisting of human beta-2 spectrin repeats 4–9. Chicken anti-MAP2 (ab5392) and anti-GFP (ab13970) antibodies were from Abcam. Mouse anti-pan NaCh (S8809), mouse anti-MAP2 (M4403), and mouse anti-calbindin (C9848) antibodies were from Sigma-Aldrich. Mouse anti-$GABA_A$ receptor β2/3 subunit (MAB341) antibody was from EMD Millipore. Guinea pig anti-VGAT (131 004) and mouse anti-gephyrin (147 021) antibodies were from Synaptic Systems. Rabbit anti-GABARAP (FL-117) antibody was from Santa Cruz. All AlexaFluor-conjugated secondary antibodies were from Life Technologies.

Neuronal Culture. Preparation of hippocampal cultures has been described (6). Hippocampi of P0 mouse pups were dissected in cold 1× Hank's Balanced Salt Solution (HBSS)/10 mM Hepes (Life Technologies) and incubated for 15–20 min at 37 °C with 0.25% trypsin and 100 μg/mL DNase (Sigma-Aldrich). Hippocampi were then washed 2× with Neurobasal-A plating medium (Life Technologies) containing 10% (vol/vol) FBS, 1× B27 supplement, 2 mM glutamine, and 1× Penicillin/Streptomycin (Pen/Strep) (Life Technologies). After wash, hippocampi were triturated by fire-polished glass pipettes, and filtered through 100-μm cell strainers to obtain dissociated cells in suspension. Cells were plated onto poly-D-lysine and laminin (Sigma-Aldrich) coated MatTek dishes. On the following day, neurons were first washed twice with plain Neurobasal-A and medium was replaced with growth medium containing B27, glutamin, Pen/Strep, and 1% FBS in Neurobasal-A. For tetrodotoxin experiments, 1 μM tetrodotoxin (Tocris Bioscience) was added to growth media after transfection and replenished every 5 d.

Transfection and Rescue. Calcium phosphate transfection was used to introduce DNA/Ca^{2+} phosphate complexes directly onto the cell layer at days 3 in vitro (DIV 3) (7). Generally, 1 μg of cDNA in a 25-μL $CaCl_2$/water solution was mixed with 2× Hank's Balanced Salt Solution followed by gentle vortexing (Clontech). The DNA-Ca^{2+}-phosphate complex was formed after incubation for 15 min at room temperature and then added dropwise to DIV 3 neurons prewashed with Neurobasal media on Mat-tek plates. Cells were incubated in a humidified 5% CO_2 chamber at 37 °C for 1 h. Precipitate was dissolved by incubating cells with Neurobasal media pre-equilibrated in 10% CO_2 in a humidified 5% CO_2 chamber at 37 °C for 20 min. Finally, cells were fed with original growth media containing 2.5 μg/mL Ara-C and maintained until DIV 21 for immunofluorescence staining as described below.

Neurons dissociated from homozygous exon 22–23 flox/flox pups were cultured as described (6). To obtain the ankyrin-G KO background, neurons were transfected with 1 μg of CAG-Cre-2A-BFP to excise ankyrin-G in vitro or -GFP plasmid as a control. For rescue experiments, 0.5 μg of CAG-Cre-2A-BFP plus 0.5 μg of CAG-GFP rescue plasmid were used. For control experiments, 1 μg of CAG-pEBFP-N1 or CAG-pEGFP-N1 plasmid was used for cell-filling in exon 22–23 flox/flox neurons.

Protein Purification and Isothermal Titration Calorimetry. N-terminal His- and C-terminal maltose binding protein double-tagged GABARAP and WT or W1989R unstructured region of 480-kDa ankyrin-G (residues 1819–2535) were expressed in BL-21 cells subject to induction with 1 mM Isopropyl β-D-1-thiogalactopyranoside (IPTG) and frozen at −80 °C overnight. On day 2, the cell pellets were solubilized and sonicated in NiNTA buffer (50 mM phosphate buffer pH 7.4, 0.3 M NaBr, 20 mM imidazole, 1 mM NaN_3, 0.5 mM EDTA, 0.5 mM DTT, 100 μg/mL AEBSF, 100 μg/mL benzamidine, 20 μg/mL leupeptin, and 10 μg/mL pepstatin) with 1% Triton X-100 and centrifuged at 100,000 × *g* at 4 °C for 1 h. The lysates were collected, incubated with NiNTA Sepharose (GE Healthcare), and rotated at 4 °C overnight. On day 3, the NiNTA resins were loaded onto columns, washed with 30 column-volume (CV) NiNTA buffer, and eluted with NiNTA buffer with 0.3 M imidazole at 2 mL per fraction. The protein-containing fractions were pooled and incubated with amylose Sepharose beads (NEB Lab) rotating at 4 °C overnight. On day 4, amylose beads were washed first with 15CV NiNTA buffer with 0.3 M imidazole and then 15 CV precision protease buffer (50 mM Tris·Cl pH 7.0, 150 mM NaCl, 1 mM EDTA, and 1 mM DTT). Beads were resuspended in equal volume of precision protease buffer with 100 units Precision Protease (GE Healthcare) at 4 °C overnight. On day 5, eluent was collected and incubated with GST beads rotating

at 4 °C for 2 h to remove Precision Protease, and the suspension was concentrated and used directly for Isothermal Titration Calorimetry.

Isothermal Titration Calorimetry (ITC) was performed by an ITC-200 (MicroCal) at 20 °C using the protocol described here (8). The concentrations of purified GABARAP and ankyrin-G insert region were calculated by Bradford Reagent (Bio-Rad) using a UV-VIS spectrophotometer (Shimadzu Scientific) at wavelength 595 nm. Cell solutions containing 20 μM WT or W1989R insert region was titrated with 30 injections of 10 μL per each syringe solution containing 200 μM GABARAP. Experiments were repeated three times to confirm the final thermodynamic parameters and stoichiometry values. The binding curves were fitted with a single site binding model in Microcal Origina software (Originlab Corporation) to obtain the binding enthalpy (ΔH), entropy (ΔS), stoichiometry (n), and the dissociation constant (K_D).

Western Blotting. Adult mice brains were dissected on ice and homogenized in 5 volume (μL)/weight (mg) buffer (0.32 M sucrose, 10 mM phosphate buffer pH 7.4, 1 mM EDTA, 1 mM NaN_3, 100 μg/mL AEBSF, 100 μg/mL benzamidine, 20 μg/mL leupeptin, and 10 μg/mL pepstatin) using a dounce homogenizer. Lysates were mixed 1:1 with 5× PAGE buffer [25% (wt/vol) sucrose, 5% (wt/vol) SDS, 50 mM Tris pH 8, 5 mM EDTA, and bromophenol blue], sonicated for 10 pulses, and heated to 65–70 °C for 10 min. Samples (10 μL/each) were loaded on a 3.5–17.5% gradient gel in 1× Tris buffer (40 mM Tris pH 7.4, 0.2% SDS, 20 mM NaOAc, and 2 mM EDTA) until the dye front diffused out of the bottom. The gel was transferred to nitrocellulose at 300 mA overnight at 4 °C in 0.5× Tris buffer (20 mM Tris pH 7.4 and 0.01% SDS). Membranes were blocked with blotting buffer (150 mM NaCl, 10 mM phosphate buffer pH 7.4, 0.2% Triton X-100, 1 mM NaN_3, and 1 mM EDTA) with 2% (wt/vol) BSA (Gemini Bioproducts) at room temperature for 1 h before incubation overnight at 4 °C with primary antibodies diluted in blocking buffer. On the next day, membranes were washed and incubated with I^{125}-labeled protein A/G 1:1,000 at room temperature for 2 h before washing and subsequent exposure on a phosphor screen. Given that protein A/G has lower affinity toward mouse IgG subclasses, membranes blotted with mouse primary antibody were incubated with a secondary rabbit anti-mouse IgG diluted 1:2,500 (Pierce) in blocking buffer before incubation with protein A/G. Radioactive signals were detected using a Typhoon imager (GE Healthcare).

Image Acquisition and Data Analysis. Samples were imaged on a Zeiss LSM 780 with a 40× 1.3 Plan-Apochromat objective and excitation was accomplished using 405-, 488-, 561-, and 633-nm lasers. Each experiment was repeated at least three independent times. Measurements were taken using Volocity (PerkinElmer) and ImageJ software. For the quantification of GABAergic synapse density, each background subtracted region of interest was drawn around the soma and proximal dendrites and converted to an 8-bit binary file. The number and the size of synaptic clusters were determined by ImageJ and normalized to the volume corresponding to each region. Conversion, threshold, and calculation parameters were kept constant for every image of each antibody staining. Statistical analysis was performed and presented using Graphpad Prism software. Data shown were mean ± SEM. Student's t test was used for comparisons between two groups, and a one-way ANOVA with Tukey post hoc test was used to compare three or more groups.

1. Kizhatil K, Bennett V (2004) Lateral membrane biogenesis in human bronchial epithelial cells requires 190-kDa ankyrin-G. *J Biol Chem* 279(16):16706–16714.
2. Jenkins PM, et al. (2014) Giant ankyrin-G was a critical innovation in vertebrate evolution of fast and integrated neuronal signaling. *Proc Natl Acad Sci USA*, 10.1073/pnas.1416544112.
3. He M, Abdi KM, Bennett V (2014) Ankyrin-G palmitoylation and βII-spectrin binding to phosphoinositide lipids drive lateral membrane assembly. *J Cell Biol* 206(2):273–288.
4. Davis JQ, Lambert S, Bennett V (1996) Molecular composition of the node of Ranvier: Identification of ankyrin-binding cell adhesion molecules neurofascin (mucin+/third FNIII domain-) and NrCAM at nodal axon segments. *J Cell Biol* 135(5):1355–1367.
5. Kizhatil K, Baker SA, Arshavsky VY, Bennett V (2009) Ankyrin-G promotes cyclic nucleotide-gated channel transport to rod photoreceptor sensory cilia. *Science* 323(5921):1614–1617.
6. He M, Tseng WC, Bennett V (2013) A single divergent exon inhibits ankyrin-B association with the plasma membrane. *J Biol Chem* 288(21):14769–14779.
7. Jiang M, Chen G (2006) High Ca2+-phosphate transfection efficiency in low-density neuronal cultures. *Nat Protoc* 1(2):695–700.
8. Wang C, Chung BC, Yan H, Lee SY, Pitt GS (2012) Crystal structure of the ternary complex of a NaV C-terminal domain, a fibroblast growth factor homologous factor, and calmodulin. *Structure* 20(7):1167–1176.

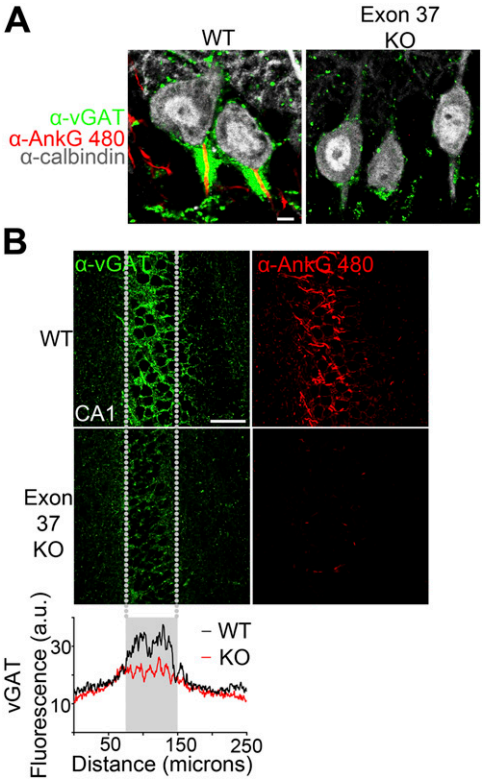

Fig. S1. 480-kDa ankyrin-G is responsible for GABAergic synapse stabilization on the Purkinje neuron AIS and hippocampal CA1 region. (*A*) Loss of vGAT staining on the AIS of exon 37 KO Purkinje neurons. (Scale bar: 5 μm.) (*B*) Reduced vGAT accumulation on the CA1 region of exon 37 KO hippocampus, as illustrated by staining (up) and quantification (bottom) of the averaged vGAT fluorescence level over 250 μm. (Scale bar: 50 μm.)

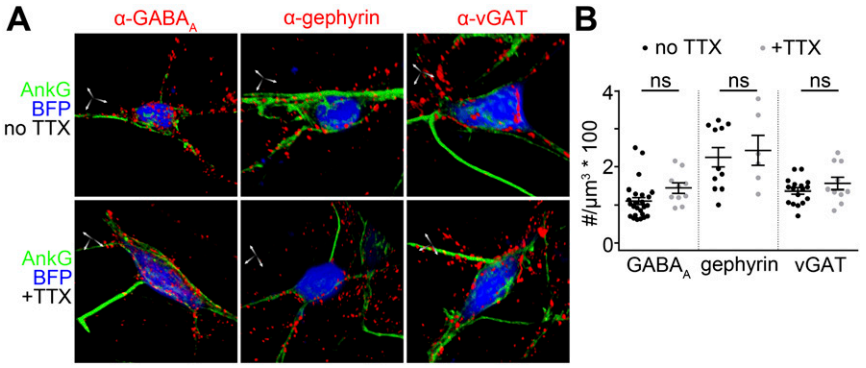

Fig. S2. Prolonged tetrodotoxin treatment does not affect the density of GABAergic synapses. (*A*) GABAA receptor, gephyrin, and vGAT still accumulate on the somatodendritic membrane and the AIS of neurons treated with TTX for 18 d. (Scale bar: 5 μm in all axes.) (*B*) The quantification of GABAergic cluster density in *A* shows no significant difference with or without TTX treatment. ns, nonsignificant (unpaired *t* test, $n = 10–15$ per group). Error bar, SEM.

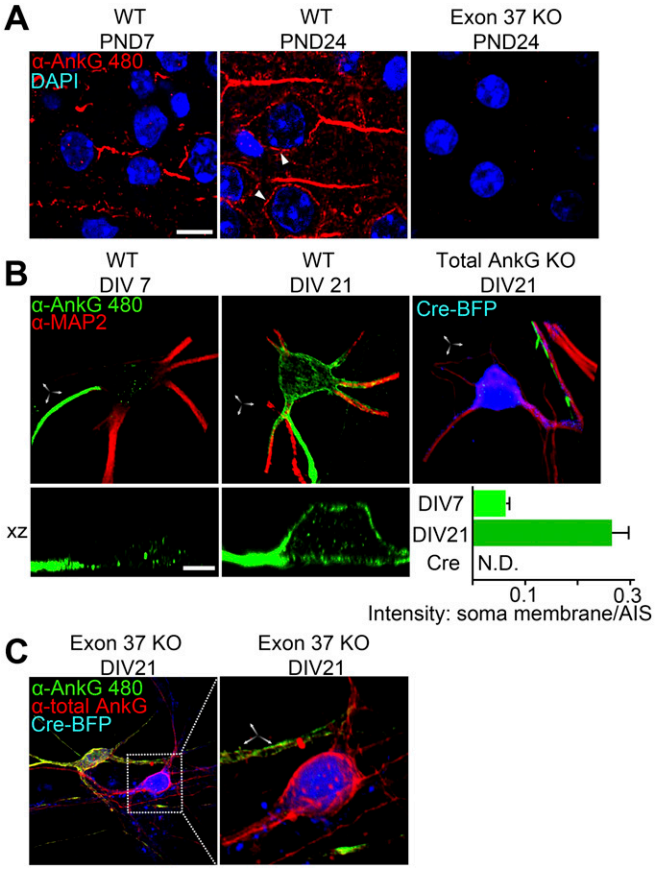

Fig. S3. Somatodendritic 480-kDa ankyrin-G is developmentally regulated in vivo and in vitro. (*A*) Somatodendritic accumulation of 480-kDa ankyrin-G only appears after PND 24 in WT cortical pyramidal neurons, whereas no 480-kDa ankyrin-G staining is detected in exon 37 KO brain. Arrowhead denotes ankyrin-G outpost on the soma. (Scale bar: 5 μm.) (*B*) In neurons dissociated from exon 22–23 flox/flox mice, 480 ankyrin-G clusters on both the AIS and somatodendritic membrane after DIV 21 in BFP-transfected neurons but not in neurons expressing Cre. (Scale bar: 5 μm in all axes.) x-z view shows the height of the somatodendritic membrane delineated by 480-kDa ankyrin-G staining (left). The ratio of somatodendritic membrane to the AIS at different developmental stages is quantified (right). (Scale bar: 5 μm.) (*C*) The remaining staining from the antibody against total ankyrin-G in exon 37 KO neurons indicates the presence of 190-kDa ankyrin-G on the somatodendritic membrane. Dotted box shows the region of magnified soma. (Scale bar: 5 μm in all axes.)

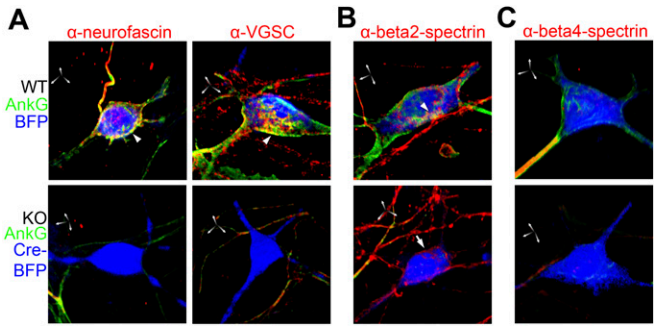

Fig. S4. Ankyrin-G is required for the somatodendritic localization of voltage-gated sodium channel and neurofascin but not spectrins. (*A*) Both VGSC and neurofascin accumulate on the somatodendritic membrane as well as the AIS of WT neurons but not ankyrin-G KO neurons. Arrowheads indicate neurofascin or VGSC outposts on the soma of WT neurons. (*B*) Beta-2 spectrin also exists on the somatodendritic membrane, whereas its accumulation persists in ankyrin-G KO neurons. Arrowhead denotes beta-2 spectrin clusters on the soma of the WT neuron, and the arrow marks the presence of beta-2 spectrin on the soma of an ankyrin-G KO neuron. C, Beta-4 spectrin only concentrates on the AIS of the WT neuron. (Scale bar: 5 μm in all axes.)

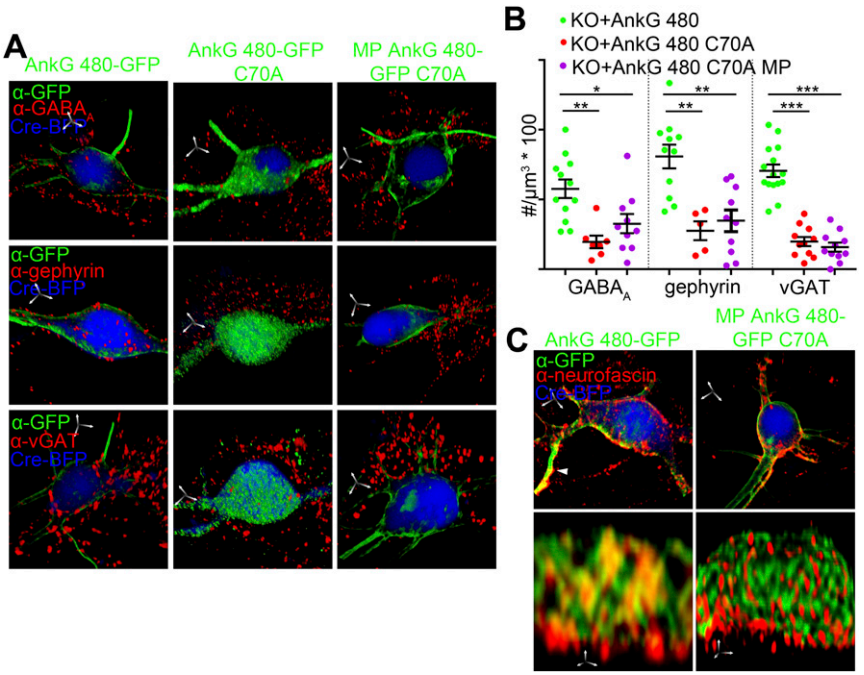

Fig. S5. Both the association of Ankyrin-G with plasma membrane and the formation of specific microdomains are required for GABAergic synapse stability. (*A*) C70A 480-kDa ankyrin-G and MP C70A 480-kDa ankyrin-G were both unable to rescue the clustering of $GABA_A$ receptor, gephyrin, or vGAT. (Scale bar: 5 μm in all axes.) (*B*) Quantification of *A*. $*P < 0.05$. $**P < 0.005$. $***P < 0.0005$ (unpaired *t* test, $n = 10–15$ per group). Error bar, SEM. (*C*) In contrast to WT 480-kDa ankyrin-G which colocalizes with neurofascin on the somatodendritic plasma membrane, MP C70A 480-kDa ankyrin-G does not form functional microdomains as suggested by the loss of neurofascin colocalization.

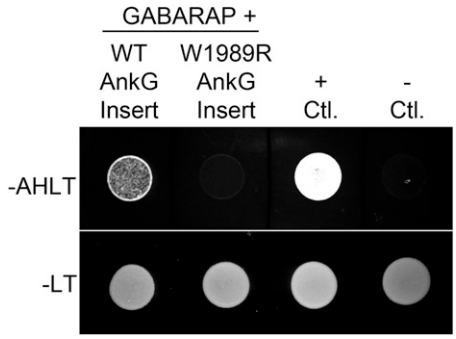

Fig. S6. Yeast two-hybrid assay identifies GABARAP as potential binding partner of insert region. A representative yeast two-hybrid assay demonstrates the binding between full length GABARAP and the residues 1479–2337 in 480-kDa ankyrin-G. The point mutation W1989R in residue 1479–2337 abolishes the interaction with GABARAP. Positive (RanBPM + pGAD) and negative control (T7 + pGAD) are shown on the right. (*Upper*) Minus AHLT plate. (*Lower*) Minus LT plate.

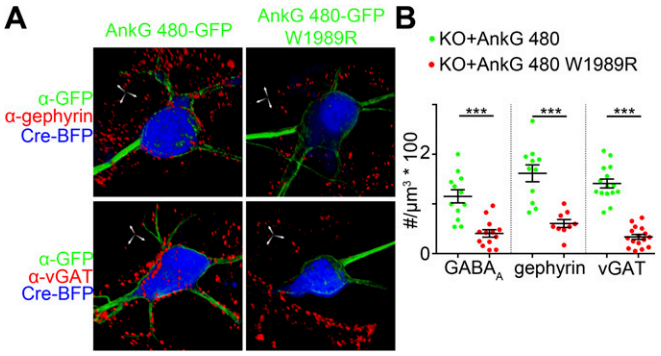

Fig. S7. W1989R 480-kDa ankyrin-G cannot rescue the GABAergic clustering on the membrane of ankyrin-G KO neurons. (*A*) In contrast to the restoration of GABAergic innervations with WT 480-kDa ankyrin-G, W1989R 480-kDa ankyrin-G fails to accumulate gephyrin or vGAT on the somatodendritic membrane and the AIS of ankyrin-G KO neurons. (Scale bar: 5 μm in all axes.) (*B*) Quantification of *A* including results from Fig. 3. ***$P < 0.0005$ (unpaired *t* test, $n = 10–15$ per group). Error bar, SEM.

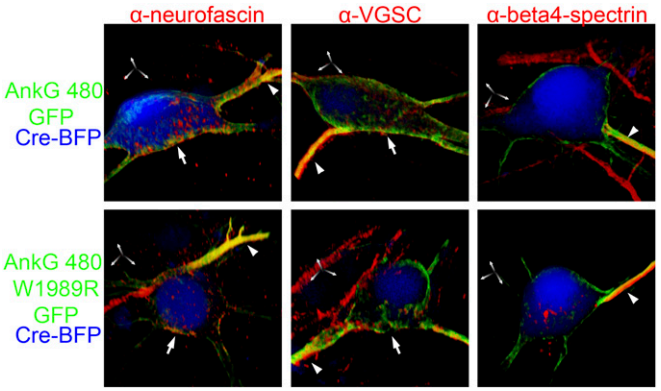

Fig. S8. W1989R 480-kDa ankyrin-G fully restores AIS proteins on the somatodendritic membrane and the functional AIS of ankyrin-G KO neurons. W1989R 480-kDa ankyrin-G accumulates VGSC, neurofascin, and beta-4 spectrin on the AIS as well as VSGC and neurofascin on the somatodendritic membrane. Arrow heads denote proteins concentrated on the AIS as marked by ankyrin-G. Arrows indicate clusters on the somatodendritic membrane colocalized with ankyrin-G. (Scale bar: 5 μm in all axes.)

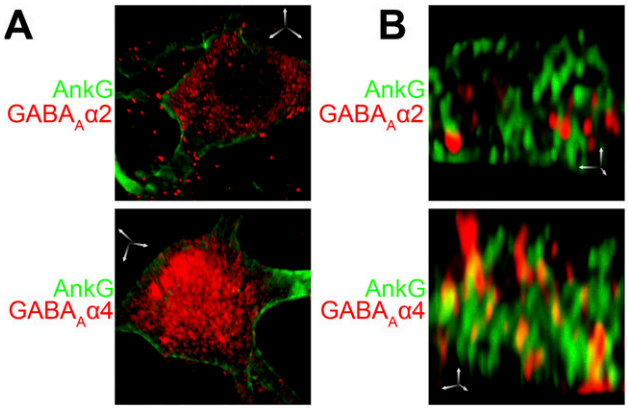

Fig. S9. Ankyrin-G colocalizes with extrasynaptic receptor subunit α4 but not synaptic subunit α2. (*A*) In WT neurons, both $GABA_A$ receptor subunits α2 and α4 appear punctate on the somatodendritic membrane. (Scale bar: 5 μm in all axes.) (Scale bar: 5 μm in all axes.) (*B*) Ankyrin-G colocalizes with extrasynaptic receptor α4 subunit in somatodendritic microdomains but is excluded from sites of synaptic receptor α2 subunit. (Scale bar: 1 μm in all axes.)

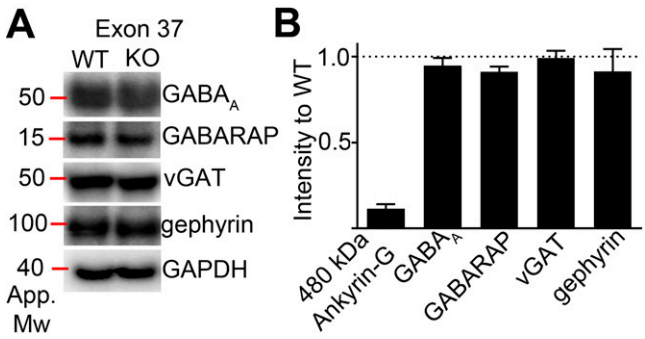

Fig. S10. The expression level of GABAergic components remains the same in exon 37 ankyrin-G KO. (*A*) The protein levels of $GABA_A$ receptor, GABARAP, vGAT, and gephyrin are not altered in exon 37 KO brain. (*B*) The quantification of band intensity shown in *A* normalized to GAPDH, with WT value set as 1. No significant difference exists between the WT and exon 37 KO brain ($n = 2$).